

# IDT: A Physically Grounded Transformer for Feed-Forward Multi-View Intrinsic Decomposition

Kang Du<sup>1</sup> Yirui Guan<sup>3</sup> Zeyu Wang<sup>1,2\*</sup>

<sup>1</sup>The Hong Kong University of Science and Technology (Guangzhou)

<sup>2</sup>The Hong Kong University of Science and Technology

<sup>3</sup>Tencent

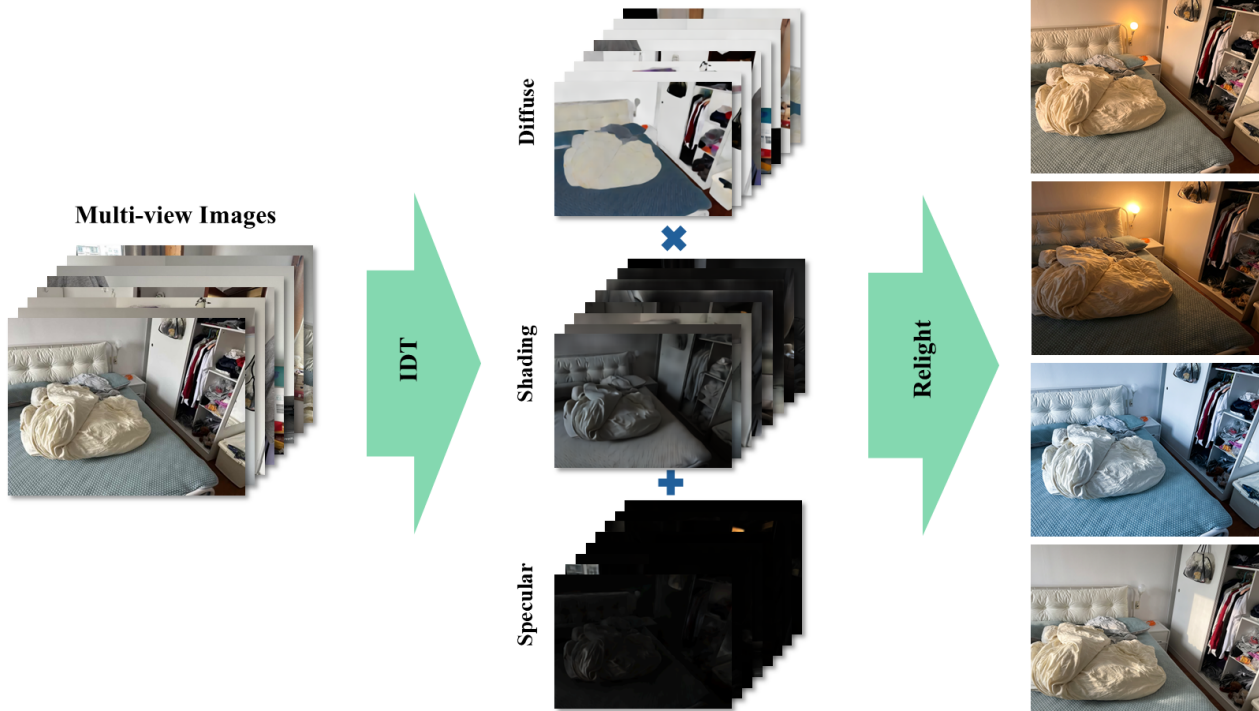


Figure 1. IDT jointly reasons over multiple views to decompose each image into diffuse reflectance, diffuse shading, and specular shading in a single feed-forward pass. These intrinsic factors faithfully reconstruct the original appearance and support relighting by altering illumination while maintaining consistent material properties across views.

## Abstract

*Intrinsic image decomposition is fundamental for visual understanding, as RGB images entangle material properties, illumination, and view-dependent effects. Recent diffusion-based methods have achieved strong results for single-view intrinsic decomposition; however, extending these approaches to multi-view settings remains challenging, often leading to severe view inconsistency. We propose **IDT**: A Physically Grounded Transformer for Feed-Forward Multi-View Intrinsic Decomposition. IDT jointly reasons over multiple input images to decompose each image into three intrinsic factors: diffuse reflectance, diffuse shading, and specular shading. These factors are then used to reconstruct the original appearance and support relighting by altering illumination while maintaining consistent material properties across views.*

***tristic Decomposition Transformer (IDT)***, a feed-forward framework for multi-view intrinsic image decomposition. By leveraging transformer-based attention to jointly reason over multiple input images, IDT produces view-consistent intrinsic factors in a single forward pass, without iterative generative sampling. IDT adopts a physically grounded image formation model that explicitly decomposes images into diffuse reflectance, diffuse shading, and specular shading. This structured factorization separates Lambertian and non-Lambertian light transport, enabling interpretable and

\*Corresponding author.

*controllable decomposition of material and illumination effects across views. Experiments on both synthetic and real-world datasets demonstrate that IDT achieves cleaner diffuse reflectance, more coherent diffuse shading, and better-isolated specular components, while substantially improving multi-view consistency compared to prior intrinsic decomposition methods. Code is available at <https://github.com/dukang/IDT>.*

## 1. Introduction

Intrinsic image decomposition seeks to factor an image into its underlying material and illumination components, offering a more interpretable and controllable representation than raw RGB appearance. Such decomposition is a long-standing goal in computer vision and graphics, and serves as a critical foundation for applications including relighting, material editing, multi-view reconstruction, and world modeling, where entangled appearance factors often hinder generalization and physical reasoning [5]. Despite decades of research, intrinsic decomposition remains fundamentally challenging due to the intertwined effects of geometry, illumination, and view-dependent appearance.

Recent years have witnessed substantial progress in intrinsic decomposition from a *single image*. Learning-based approaches, ranging from convolutional models to transformer architectures, have significantly improved per-view decomposition quality under supervised or weakly supervised settings [4]. Beyond pure RGB inputs, several methods further incorporate geometric cues such as depth or surface normals, following the broader *RGB-X* paradigm, to alleviate intrinsic ambiguities. More recently, diffusion-based models have demonstrated impressive single-view results by leveraging powerful generative priors and iterative refinement. However, a common limitation of these approaches is that they operate on each image independently, implicitly treating intrinsic decomposition as a per-view appearance generation problem.

In contrast, many downstream tasks demand *multi-view intrinsic consistency*. When multiple images of the same scene are available, independently decomposed intrinsic factors often vary across viewpoints, leading to inconsistent material appearance and unstable illumination estimates. This issue is particularly severe in indoor environments with complex lighting and view-dependent effects such as specular highlights. Such inconsistencies fundamentally limit the use of intrinsic decomposition in multi-view reconstruction, scene editing, and physically grounded world modeling. Moreover, existing iterative or generative formulations lack an explicit mechanism for jointly reasoning across multiple views, making cross-view coherence difficult to enforce.

In this work, we argue that intrinsic decomposition should be revisited from a *multi-view, feed-forward* per-

spective. Our approach builds on recent advances in transformer-based geometric reasoning, where multiple views are jointly processed to infer coherent scene representations in a single forward pass. In particular, models such as VGGT demonstrate that attention mechanisms can effectively aggregate information across views and produce consistent geometric predictions without iterative optimization [27]. This observation motivates us to extend feed-forward multi-view reasoning beyond geometry, and into the intrinsic decomposition problem.

Beyond consistency, we further emphasize the importance of *physically grounded* intrinsic representations. Rather than modeling intrinsic components as abstract latent variables or unstructured residuals, we explicitly adopt a physically motivated image formation model that decomposes appearance into *diffuse reflectance (albedo)*, *diffuse shading*, and *specular shading*. This formulation aligns with physically based rendering decompositions used in large-scale indoor datasets such as Hypersim [25], and enforces a principled separation between Lambertian and non-Lambertian effects. As a result, the predicted intrinsic factors are more interpretable, stable across viewpoints, and suitable for downstream physical reasoning.

Based on these insights, we propose **Intrinsic Decomposition Transformer (IDT)**, a feed-forward framework for multi-view intrinsic image decomposition. IDT jointly processes multiple images of a scene using transformer attention, enabling consistent inference of albedo, diffuse shading, and specular shading across views in a single forward pass. By unifying multi-view geometric reasoning with a physically grounded intrinsic formulation, IDT provides a practical and effective solution for intrinsic decomposition in realistic indoor environments.

Our contributions can be summarized as follows:

- We introduce a feed-forward transformer framework for *view-consistent* multi-view intrinsic image decomposition, extending recent advances in multi-view geometric reasoning to intrinsic factorization.
- We propose a *physically grounded* intrinsic formulation that explicitly separates diffuse reflectance, diffuse shading, and specular shading, leading to interpretable and stable intrinsic representations.
- We demonstrate improved single-view accuracy and substantially enhanced multi-view consistency on both synthetic and real-world indoor datasets compared to prior intrinsic decomposition methods.

## 2. Related Work

**Inverse rendering and physically grounded scene decomposition.** Inverse rendering aims to recover geometry, material, and illumination using explicit physical models or differentiable rendering, often trained with large-scale synthetic data [1, 2, 6, 10, 13, 14, 19, 22, 24, 26, 32–35]. These

approaches provide strong physical interpretability and enable downstream tasks such as relighting and view synthesis. However, they typically rely on iterative optimization, volumetric rendering, or explicit scene representations, leading to high computational cost and limited scalability. As a result, they are not well suited for efficient, feed-forward intrinsic factorization directly from multi-view images.

**Intrinsic image decomposition.** Intrinsic image decomposition seeks to separate reflectance and illumination-related factors from images without explicitly reconstructing full scene geometry. Classical Retinex-based formulations [3, 16, 17, 31, 37, 39] and benchmark datasets [11] establish the foundational problem setting and highlight its inherent ambiguity. Learning-based approaches [4, 23, 36] significantly improve visual quality by directly regressing intrinsic components. Nevertheless, most methods perform per-image inference and treat intrinsic factors independently across views, making it difficult to maintain consistency under view-dependent effects or multi-view observations.

**Diffusion-based intrinsic decomposition.** Recently, diffusion models have been adopted as powerful generative priors for intrinsic decomposition and material estimation [9, 15, 18]. By modeling the distribution of plausible intrinsic solutions, these methods achieve strong performance in ambiguous single-view settings. Despite their effectiveness, diffusion-based approaches require iterative sampling at inference time and operate independently on each image, which limits their efficiency, scalability, and ability to enforce cross-view consistency in multi-view scenarios.

**Multi-view reasoning and feed-forward transformers.** Multi-view vision has been significantly advanced by neural scene representations such as NeRF [21], which enable high-quality novel view synthesis from sparse observations. However, such methods rely on volumetric rendering and per-scene optimization and are not designed for direct intrinsic decomposition. More recent feed-forward transformer architectures [20, 27, 28, 30, 40] demonstrate that multi-view information can be aggregated efficiently in a single forward pass. While effective for geometry or view synthesis, existing methods do not explicitly model intrinsic image factors or the separation of material and illumination, leaving multi-view intrinsic decomposition largely unexplored.

### 3. Method

We propose **Intrinsic Decomposition Transformer (IDT)**, a feed-forward framework for physically grounded intrinsic image decomposition from multiple views. Given a set of images observing the same static scene from different viewpoints, IDT jointly infers view-consistent intrinsic factors under an explicit image formation model. Our design is motivated by a key observation: intrinsic decomposition fundamentally differs from geometric reconstruction. While geometry benefits from aggregating all cross-view correspondences, intrinsic factors require *selective* reasoning over appearance, illumination, and view-dependent effects. IDT addresses this challenge by combining multi-view transformer aggregation with factor-specific appearance adapters, as shown in Figure 2.

#### 3.1. Problem Formulation and Image Formation Model

We study intrinsic image decomposition in a multi-view setting. Given a set of  $V$  images

$$\mathcal{I} = \{\mathbf{I}_v\}_{v=1}^V, \quad (1)$$

captured from different viewpoints observing the same static scene, our goal is to recover intrinsic factors that explain material appearance and illumination while remaining consistent across views.

**Image formation model.** We adopt a physically grounded image formation model that separates Lambertian and non-Lambertian light transport. For each view  $v$ , the observed image is modeled as

$$\mathbf{I}_v(\mathbf{x}) = \mathbf{A}(\mathbf{x}) \odot \mathbf{S}_v^{\text{diff}}(\mathbf{x}) + \mathbf{S}_v^{\text{spec}}(\mathbf{x}), \quad (2)$$

where  $\mathbf{A}$  denotes view-invariant diffuse reflectance (albedo),  $\mathbf{S}_v^{\text{diff}}$  denotes diffuse shading capturing illumination-dependent Lambertian effects, and  $\mathbf{S}_v^{\text{spec}}$  models view-dependent non-Lambertian effects such as specular highlights.

This formulation follows a standard rendering approximation widely adopted in intrinsic image decomposition and inverse rendering. Under a diffuse–specular BRDF decomposition, the rendering equation is linear in reflectance, yielding an additive separation between diffuse and specular contributions [2, 24]. Assuming Lambertian diffuse reflectance causes the diffuse term to factorize into a view-invariant albedo and a view-dependent irradiance term, motivating the multiplicative form  $\mathbf{A} \odot \mathbf{S}_v^{\text{diff}}$  [3, 17]. In contrast, specular reflection depends strongly on view direction and microfacet alignment, and cannot be reliably factorized without explicit BRDF parameters such as roughness [8]. We therefore model it as an additive, view-dependent component. Explicitly isolating specular effects prevents view-dependent appearance from leaking into albedo, which is

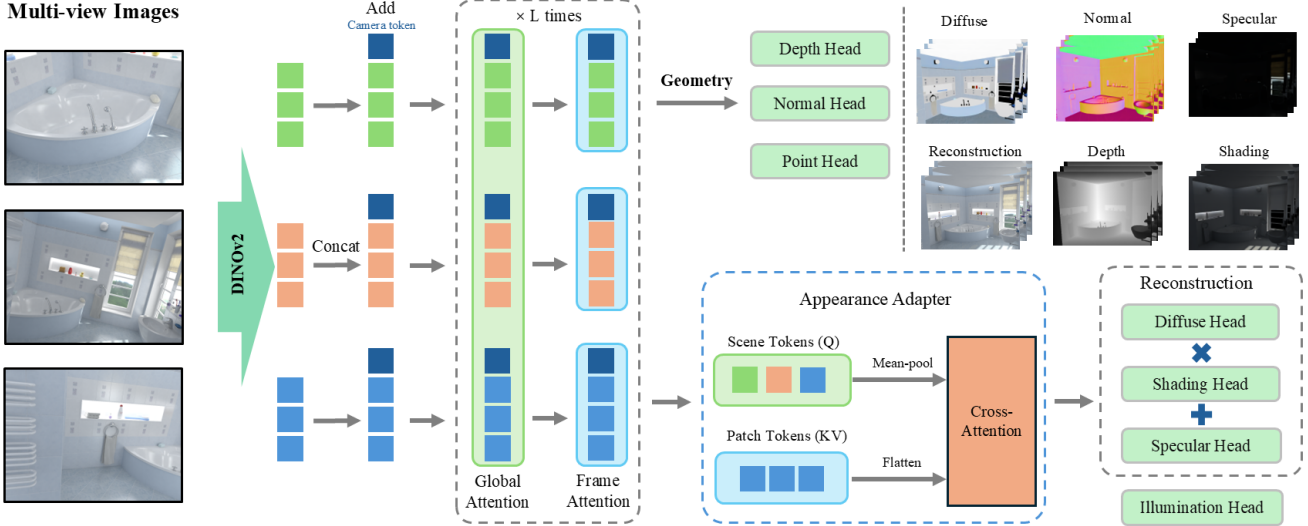


Figure 2. Overview of the IDT pipeline. Given multiple images of a static scene, IDT first aggregates cross-view information using a multi-view transformer encoder. The shared latent tokens are then selectively routed by factor-specific appearance adapters to predict view-invariant albedo, view-dependent diffuse and specular shading, and a shared scene-level illumination representation. All intrinsic factors are inferred in a single feed-forward pass and are jointly constrained by a physically grounded image formation model.

a primary source of inconsistency in per-view intrinsic decomposition.

**Illumination representation.** Intrinsic decomposition is inherently coupled with illumination. To capture shared lighting structure across views, we introduce a compact scene-level illumination representation parameterized as a *Spherical Gaussian Mixture (SGM)*. Spherical Gaussians provide an efficient and differentiable approximation of environment lighting and have been widely used in inverse rendering and neural relighting [24]. Rather than performing explicit physically based rendering, this representation is used as a conditioning signal for shading prediction, avoiding the need for explicit BRDF parameters such as roughness.

### 3.2. Feed-Forward Multi-View Intrinsic Decomposition

Instead of decomposing each image independently, IDT performs joint inference over all views in a single forward pass. Formally, given the multi-view input  $\mathcal{I}$ , the model predicts

$$\mathcal{F} = \{\mathbf{A}, \{\mathbf{S}_v^{\text{diff}}\}_{v=1}^V, \{\mathbf{S}_v^{\text{spec}}\}_{v=1}^V, \mathbf{L}\}, \quad (3)$$

where albedo  $\mathbf{A}$  and illumination  $\mathbf{L}$  are shared across all views, while shading components remain view-dependent. This feed-forward formulation enforces cross-view consistency at the representation level and avoids iterative generative inference commonly used in prior intrinsic and inverse rendering approaches, as shown in Figure 3.

### 3.3. Emergent Geometry–Appearance Token Specialization

To enable joint reasoning across views, we adopt a VGGT-style multi-view transformer encoder. Given the input images  $\mathcal{I}$ , the encoder produces a single set of latent tokens

$$\mathbf{Z} = \mathcal{E}(\mathcal{I}). \quad (4)$$

Importantly, IDT does not explicitly partition  $\mathbf{Z}$  into geometry and appearance tokens. Instead, geometry–appearance specialization emerges implicitly through task-specific supervision and routing. During training, tokens that are strongly supervised by geometric objectives (e.g., depth, surface normal, or camera estimation) become specialized for geometric reasoning, while other tokens are primarily shaped by intrinsic decomposition losses and encode appearance-related information such as material and illumination cues. We conceptually denote these roles as  $\mathbf{Z}^{\text{geo}}$  and  $\mathbf{Z}^{\text{app}}$ , while emphasizing that this distinction arises from training dynamics rather than hard token splitting. This design preserves the flexibility of transformer representations and is consistent with emergent token specialization observed in multi-task transformer models [7].

### 3.4. Appearance Adapters for Intrinsic Prediction

Appearance-related representations produced by the multi-view transformer are expressive but highly redundant. In multi-view intrinsic decomposition, different intrinsic factors rely on distinct and partially conflicting cues: diffuse reflectance (albedo) should emphasize view-invariant material properties, whereas diffuse and specular shading are



Figure 3. Illustration of the physically grounded image formation model. For each view, the observed image is decomposed into a view-invariant diffuse reflectance, a view-dependent shading term modeling Lambertian illumination, and an additive view-dependent specular component capturing non-Lambertian effects. This formulation yields a multiplicative separation between albedo and diffuse shading and explicitly isolates specular appearance to prevent view-dependent effects from leaking into material properties.

strongly influenced by view-dependent effects, lighting direction, and global illumination. Directly feeding the same shared token set into all prediction heads therefore tends to entangle material and illumination cues, often resulting in color leakage in albedo or unstable shading predictions across views.

To enable selective and factor-specific reasoning, we introduce *appearance adapters* that explicitly route information from the shared multi-view token set to each intrinsic prediction head. Rather than enforcing a single shared representation, the adapters act as lightweight interfaces that extract task-relevant appearance information while suppressing irrelevant or conflicting cues. For each intrinsic factor  $k \in \{\text{alb, diff, spec}\}$ , an adapter produces a compact, task-specific representation:

$$\tilde{\mathbf{Z}}_k = \mathcal{A}_k(\mathbf{Z}), \quad (5)$$

where  $\mathbf{Z}$  denotes the aggregated multi-view tokens output by the encoder.

**Scene-conditioned cross-attention.** Each appearance adapter  $\mathcal{A}_k$  is implemented as a lightweight cross-attention block. Crucially, the queries are *not learnable parameters* but are derived directly from the encoder outputs. Specifically, we construct queries by pooling scene-level tokens (e.g., camera tokens and register tokens) across views, which encode global scene geometry and camera configuration. Keys and values are formed from patch-level tokens across all views, representing dense multi-view appearance observations. This asymmetric design allows scene-level representations to selectively attend to relevant appearance cues distributed over multiple views.

By conditioning attention on scene tokens rather than learned slots, the adapter remains fully feed-forward and avoids introducing additional latent variables or iterative optimization. Moreover, because the queries encode scene-level geometry and camera information, the resulting attended features are naturally aligned across views, yielding

a scene-conditioned context that is consistent under viewpoint changes. This design encourages the albedo adapter to focus on view-invariant material properties, while allowing the shading adapters to aggregate view-dependent illumination cues in a controlled manner.

**Factor-specific decoupling.** Although all appearance adapters share the same architectural form, their parameters are factor-specific and not shared across intrinsic heads. This design allows each adapter to learn distinct attention patterns tailored to its target factor. In practice, we observe that the albedo adapter assigns higher attention weights to geometrically stable regions across views, whereas the diffuse and specular shading adapters attend more strongly to view-dependent highlights and illumination variations. As a result, the adapters effectively decouple material and illumination information before prediction, reducing cross-factor interference and improving both single-view accuracy and multi-view consistency.

**Relation to adapter-based learning.** Conceptually, our appearance adapters are related to task-specific routing and adapter modules used in multi-task transformer learning [12], but differ in that they operate over structured multi-view token sets and use scene-derived queries rather than additional learnable parameters. This makes them particularly well suited for intrinsic decomposition, where factors share a common scene context but require different appearance cues.

Using the adapted representations, intrinsic factors are predicted as

$$\mathbf{A} = h_{\text{alb}}(\tilde{\mathbf{Z}}_{\text{alb}}), \quad (6)$$

$$\mathbf{S}_v^{\text{diff}} = h_{\text{diff}}(\tilde{\mathbf{Z}}_{\text{diff}, v}, \mathbf{L}), \quad (7)$$

$$\mathbf{S}_v^{\text{spec}} = h_{\text{spec}}(\tilde{\mathbf{Z}}_{\text{spec}, v}, \mathbf{L}), \quad (8)$$

where  $\mathbf{L}$  denotes the shared Spherical Gaussian Mixture (SGM) illumination representation. Conditioning shading heads on  $\mathbf{L}$  enables illumination-aware prediction without enforcing explicit physically based rendering equations.

### 3.5. Training Objectives

We supervise intrinsic factors using loss functions consistent with their physical interpretations. When ground-truth intrinsic layers are available, we apply direct supervision on each factor; otherwise, learning is regularized through image reconstruction under the proposed image formation model.

#### Albedo loss.

$$\mathcal{L}_{\text{alb}} = \|\mathbf{A} - \mathbf{A}^*\|_1, \quad (9)$$

where  $\mathbf{A} \in \mathbb{R}^{H \times W \times 3}$  denotes the predicted view-invariant diffuse reflectance (albedo),  $\mathbf{A}^*$  is the corresponding ground truth when available, and  $\|\cdot\|_1$  is the element-wise  $\ell_1$  norm over spatial locations and color channels. We adopt an  $\ell_1$  loss to preserve sharp material boundaries and reduce color bleeding.

#### Diffuse shading loss.

$$\mathcal{L}_{\text{diff}} = \|\log(\mathbf{S}^{\text{diff}} + \epsilon) - \log(\mathbf{S}^{\text{diff}*} + \epsilon)\|_2^2, \quad (10)$$

where  $\mathbf{S}_v^{\text{diff}} \in \mathbb{R}^{H \times W \times 3}$  denotes the predicted diffuse shading (irradiance) for view  $v$ ,  $\mathbf{S}_v^{\text{diff}*}$  is the ground truth,  $\epsilon$  is a small constant for numerical stability, and  $\|\cdot\|_2^2$  denotes the squared  $\ell_2$  norm. The logarithmic formulation emphasizes relative intensity errors and is robust to global illumination scale changes.

#### Specular shading loss.

$$\mathcal{L}_{\text{spec}} = \|\log(\mathbf{S}^{\text{spec}} + \epsilon) - \log(\mathbf{S}^{\text{spec}*} + \epsilon)\|_2^2, \quad (11)$$

where  $\mathbf{S}_v^{\text{spec}}$  denotes the predicted view-dependent specular component for view  $v$  and  $\mathbf{S}_v^{\text{spec}*}$  is the corresponding supervision when available. This loss prevents sparse, high-intensity highlights from dominating training and encourages a clean separation between diffuse and non-Lambertian effects.

#### Reconstruction loss.

$$\mathcal{L}_{\text{recon}} = \frac{1}{V} \sum_{v=1}^V \|\mathbf{A} \odot \mathbf{S}_v^{\text{diff}} + \mathbf{S}_v^{\text{spec}} - \mathbf{I}_v\|_1, \quad (12)$$

where  $V$  is the number of input views,  $\mathbf{I}_v$  is the observed RGB image for view  $v$ , and  $\odot$  denotes element-wise multiplication. This term enforces consistency with the image formation model and regularizes intrinsic predictions when explicit supervision is incomplete or unavailable.

#### Illumination loss.

$$\mathcal{L}_{\text{illum}} = \|\mathbf{L} - \mathbf{L}^*\|_2^2, \quad (13)$$

where  $\mathbf{L}$  denotes the predicted scene-level illumination parameters (e.g., Spherical Gaussian Mixture coefficients) and  $\mathbf{L}^*$  is the corresponding ground truth when available. This loss is applied only on datasets with explicit illumination supervision.

**Overall objective.** The final training objective is a weighted sum of all loss terms:

$$\mathcal{L} = \lambda_{\text{alb}} \mathcal{L}_{\text{alb}} + \lambda_{\text{diff}} \mathcal{L}_{\text{diff}} + \lambda_{\text{spec}} \mathcal{L}_{\text{spec}} + \lambda_{\text{recon}} \mathcal{L}_{\text{recon}} + \lambda_{\text{illum}} \mathcal{L}_{\text{illum}}, \quad (14)$$

where  $\lambda$  are scalar weights balancing the contributions of different objectives.

## 4. Experiments

We evaluate the proposed Intrinsic Decomposition Transformer (IDT) from two complementary perspectives: (i) **single-view intrinsic and geometric prediction quality**, and (ii) **multi-view consistency of the predicted factors**. This experimental design explicitly disentangles per-view estimation accuracy from cross-view coherence, which is critical for physically meaningful intrinsic decomposition.

### 4.1. Datasets

**Hypersim.** Hypersim [25] is a large-scale synthetic indoor dataset with physically based rendering and full intrinsic ground truth, including depth, surface normals, diffuse reflectance, diffuse illumination, and non-Lambertian residuals. We use Hypersim as the primary benchmark for quantitative evaluation of single-view accuracy and multi-view consistency under controlled supervision.

**InteriorVerse.** InteriorVerse [38] contains real-world or photorealistic indoor scenes with complex geometry, materials, and lighting. While full intrinsic ground truth is unavailable, InteriorVerse serves as a challenging testbed for evaluating generalization, visual quality, and cross-view consistency in realistic scenarios.

For both datasets, we construct multi-view samples by grouping  $V$  images captured from nearby viewpoints of the same static scene.

### 4.2. Evaluation Metrics

**Single-view prediction accuracy.** For depth and surface normals, we report standard geometric metrics, including absolute relative error (AbsRel), root mean square error (RMSE), and mean angular error for normals. For intrinsic factors (albedo and shading), we evaluate MAE, PSNR, and SSIM. Shading-related metrics are additionally computed in the logarithmic domain to account for high dynamic range.

**Multi-view consistency.** To evaluate cross-view consistency, we warp predicted intrinsic factors (albedo, shading, and normals) from each view to a reference view using known camera geometry. We then compute the average  $\ell_1$  difference between warped predictions. Lower values indicate better multi-view consistency.

**Reconstruction quality.** We additionally evaluate image reconstruction quality by recomposing the input image using the predicted intrinsic factors according to Eq. (2). PSNR and SSIM are reported on both Hypersim and InteriorVerse.

Table 1. Single-view intrinsic decomposition results on HyperSim.

Method	Albedo PSNR $\uparrow$	Albedo MAE $\downarrow$	Albedo SSIM $\uparrow$	Shading PSNR $\downarrow$	Shading SSIM $\uparrow$
IID	15.42	0.061	0.781	-	-
RGBX	21.10	0.024	0.742	15.42	0.734
<b>IDT (Ours)</b>	<b>22.85</b>	<b>0.021</b>	<b>0.842</b>	<b>18.32</b>	<b>0.801</b>

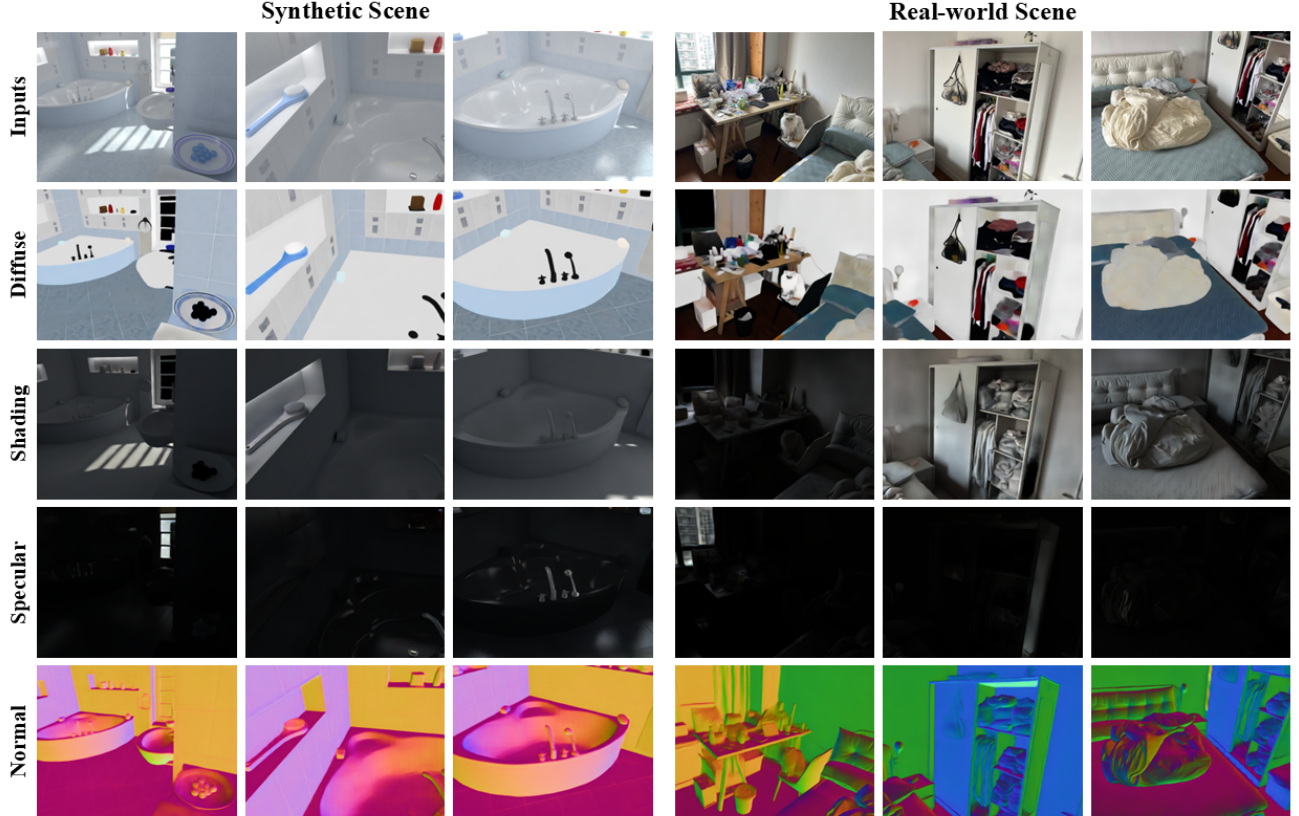


Figure 4. Qualitative intrinsic decomposition and geometry prediction results. IDT performs feed-forward inference to predict depth, surface normals, diffuse reflectance (albedo), and diffuse shading from one or multiple views. Compared to existing single-view and multi-view baselines, IDT produces sharper geometry, cleaner intrinsic factors, and substantially improved cross-view consistency.

Table 2. Single-view depth estimation results.

Method	AbsRel $\downarrow$	RMSE $\downarrow$	$\delta_1 \uparrow$
Depth Anything	0.406	0.391	0.372
VGGT	0.383	0.354	0.412
<b>IDT (Ours)</b>	<b>0.358</b>	<b>0.341</b>	<b>0.433</b>

Table 3. Single-view surface normal estimation results.

Method	Mean Angular Error $\downarrow$	$11.25^\circ \uparrow$
RGB-X	19.8	58.8
<b>IDT (Ours)</b>	<b>14.1</b>	<b>60.8</b>

### 4.3. Baselines

We compare IDT against strong baselines tailored to each prediction task.

**Depth estimation.** We compare against Depth Anything [29], VGGT [27], which represent state-of-the-art single-view depth estimation methods. All baselines are evaluated in a single-view setting.

**Surface normal estimation.** We compare against RGB-X based normal estimation methods [31] and intrinsic image decomposition (IID) [15] based approaches, which jointly reason about reflectance and shading cues for normal prediction.

**Intrinsic image decomposition.** For albedo and shading, we compare against representative intrinsic decomposition methods, including IID models and recent learning-based approaches. All single-view baselines are applied independently to each view.

**Multi-view baselines.** To evaluate multi-view consistency, all single-view baselines are extended by independently processing each view, followed by geometric warping. In addition, we include a per-view VGGT baseline that shares the same backbone and training setup as IDT but without joint multi-view attention, allowing us to isolate the effect of joint inference.

#### 4.4. Baselines

We compare IDT against strong baselines tailored to each prediction task.

**Depth estimation.** We compare against Depth Anything [29], VGGT [27], which represent state-of-the-art single-view depth estimation methods. All baselines are evaluated in a single-view setting.

**Surface normal estimation.** We compare against RGB-X based normal estimation methods [31] and intrinsic image decomposition (IID) based approaches, which jointly reason about reflectance and shading cues for normal prediction.

**Intrinsic image decomposition.** For albedo and shading, we compare against representative intrinsic decomposition methods, including IID-based models and recent learning-based approaches. All single-view baselines are applied independently to each view.

**Multi-view baselines.** To evaluate multi-view consistency, all single-view baselines are extended by independently processing each view, followed by geometric warping. In addition, we include a per-view VGGT baseline that shares the same backbone and training setup as IDT but without joint multi-view attention, allowing us to isolate the effect of joint inference.

#### 4.5. Quantitative Results

**Single-view results.** Single-view quantitative comparisons are reported in Tables 2, 3, and 1. IDT consistently matches or outperforms state-of-the-art methods on depth, surface normals, and intrinsic decomposition, demonstrating that joint modeling does not compromise per-view accuracy.

#### 4.6. Ablation Studies

We conduct ablation studies on Hypersim to analyze key components of IDT.

**Joint multi-view inference.** Removing joint multi-view attention and processing each view independently leads to a significant degradation in cross-view consistency, while single-view accuracy remains comparable.

**Intrinsic adapters.** Disabling intrinsic-specific adapters results in increased entanglement between material and illumination factors, leading to degraded albedo and shading quality.

**Illumination conditioning.** Removing SGM-based illumination conditioning leads to unstable shading estimates and increased illumination leakage into albedo.

#### 4.7. Qualitative Results

Figure 4 shows qualitative results on Hypersim and InteriorVerse. IDT produces sharper depth, cleaner normals, and more coherent albedo and shading across views. Compared to baselines, IDT better isolates non-Lambertian effects and maintains consistent intrinsic factors under viewpoint changes.

### 5. Conclusion

**Limitations.** IDT relies on a simplified image formation model and may be challenged by extreme lighting conditions or strongly non-Lambertian materials. In addition, the current approach does not explicitly enforce global geometric constraints and is primarily evaluated on indoor scenes.

We introduced Intrinsic Decomposition Transformer (IDT), a feed-forward framework for physically grounded multi-view intrinsic image decomposition. By jointly reasoning over multiple views with transformer attention, IDT infers view-consistent intrinsic factors in a single forward pass without iterative inference. An explicit image formation model that separates diffuse reflectance, diffuse shading, and specular effects further improves the disentanglement of material and illumination. Experiments on synthetic and real-world indoor datasets demonstrate that IDT produces cleaner intrinsic decompositions and substantially improved multi-view consistency over prior methods.

## References

- [1] Jonathan T. Barron and Jitendra Malik. Shape, illumination, and reflectance from shading. In *Proceedings of the European Conference on Computer Vision (ECCV)*, 2012. 2
- [2] Jonathan T. Barron and Jitendra Malik. Shape, illumination, and reflectance from shading. *IEEE Transactions on Pattern Analysis and Machine Intelligence*, 2015. 2, 3
- [3] Harry G. Barrow and Jay M. Tenenbaum. Recovering intrinsic scene characteristics from images. In *Computer Vision Systems*. 1978. 3
- [4] Anil S. Baslamisli, Timo Groenestege, S. Das, and Theo Gevers. All about intrinsics: A comprehensive study of intrinsic image decomposition. In *Proceedings of the IEEE/CVF Conference on Computer Vision and Pattern Recognition (CVPR)*, 2018. 2, 3
- [5] Sean Bell, Kavita Bala, and Noah Snavely. Intrinsic images in the wild. *ACM Transactions on Graphics*, 33(4), 2014. 2
- [6] Sai Bi, Zexiang Xu, Pratul Srinivasan, Ben Mildenhall, Kalyan Sunkavalli, Miloš Hašan, Yannick Hold-Geoffroy, David Kriegman, and Ravi Ramamoorthi. Neural Reflectance Fields for Appearance Acquisition. *arXiv preprint arXiv:2008.03824*, 2020. 2
- [7] Nicolas Carion, Francisco Massa, Gabriel Synnaeve, Nicolas Usunier, Alexander Kirillov, and Sergey Zagoruyko. End-to-end object detection with transformers. In *Proceedings of the European Conference on Computer Vision (ECCV)*, 2020. 4
- [8] Robert L. Cook and Kenneth E. Torrance. A reflectance model for computer graphics. *ACM Transactions on Graphics*, 1(1):7–24, 1982. 3
- [9] Hala Djeghem, Nathan Piasco, Luis Roldão, Moussab Ben-nehar, Dzmitry Tsishkou, Céline Loscos, and Désiré Sidibé. Sail: Self-supervised albedo estimation from real images with a latent diffusion model, 2025. 3
- [10] Kang Du, Zhihao Liang, and Zeyu Wang. Gs-id: Illumination decomposition on gaussian splatting via diffusion prior and parametric light source optimization, 2024. 2
- [11] Roger Grosse, Micah K. Johnson, Edward H. Adelson, and William T. Freeman. Ground truth dataset and baseline evaluations for intrinsic image algorithms. In *Proceedings of the IEEE International Conference on Computer Vision (ICCV)*, 2009. 3
- [12] Neil Houlsby, Andrei Giurgiu, Stanislaw Jastrzebski, et al. Parameter-efficient transfer learning for nlp. In *Proceedings of the International Conference on Machine Learning (ICML)*, 2019. 5
- [13] Yingwenqi Jiang, Jiadong Tu, Yuan Liu, Xifeng Gao, Xiaoxiao Long, Wenping Wang, and Yuexin Ma. GaussianShader: 3D Gaussian Splatting With Shading Functions for Reflective Surfaces. In *Proceedings of the IEEE/CVF Conference on Computer Vision and Pattern Recognition*, pages 5322–5332, 2024. 2
- [14] Haian Jin, Isabella Liu, Peijia Xu, Xiaoshuai Zhang, Songfang Han, Sai Bi, Xiaowei Zhou, Zexiang Xu, and Hao Su. Tensoir: Tensorial inverse rendering. In *Proceedings of the IEEE/CVF Conference on Computer Vision and Pattern Recognition*, pages 165–174, 2023. 2
- [15] Peter Kocsis, Vincent Sitzmann, and Matthias Nießner. Intrinsic image diffusion. *arXiv preprint arXiv:2312.12274*, 2023. 3, 8
- [16] Peter Kocsis, Vincent Sitzmann, and Matthias Nießner. Intrinsic image diffusion for indoor single-view material estimation. In *Proceedings of the IEEE/CVF Conference on Computer Vision and Pattern Recognition*, pages 5198–5208, 2024. 3
- [17] Edwin H. Land and John J. McCann. Lightness and retinex theory. *Journal of the Optical Society of America*, 61(1):1–11, 1971. 3
- [18] Zhibing Li, Tong Wu, Jing Tan, Mengchen Zhang, Jiaqi Wang, and Dahua Lin. IDarb: Intrinsic decomposition for arbitrary number of input views and illuminations. In *The Thirteenth International Conference on Learning Representations*, 2025. 3
- [19] Zhihao Liang, Qi Zhang, Ying Feng, Ying Shan, and Kui Jia. Gs-ir: 3d gaussian splatting for inverse rendering. *CoRR*, abs/2311.16473, 2023. 2
- [20] Dominic Maggio, Hyungtae Lim, and Luca Carlone. Vggt-slam: Dense rgb slam optimized on the sl (4) manifold. *Advances in Neural Information Processing Systems*, 39, 2025. 3
- [21] Ben Mildenhall, Pratul P. Srinivasan, Matthew Tancik, Jonathan T. Barron, Ravi Ramamoorthi, and Ren Ng. Nerf: Representing scenes as neural radiance fields for view synthesis. In *Proceedings of the European Conference on Computer Vision (ECCV)*, 2020. 3
- [22] Jacob Munkberg, Jon Hasselgren, Tianshang Shen, Jun Gao, Wenzheng Chen, Alex Evans, Thomas Müller, and Sanja Fidler. Extracting Triangular 3D Models, Materials, and Lighting From Images. In *Proceedings of the IEEE/CVF Conference on Computer Vision and Pattern Recognition*, pages 8280–8290, 2022. 2
- [23] Takuya Narihira, Michael Maire, and Stella X. Yu. Direct intrinsics: Learning albedo-shading decomposition by convolutional regression. In *Proceedings of the IEEE International Conference on Computer Vision (ICCV)*, 2015. 3
- [24] Ravi Ramamoorthi and Pat Hanrahan. A signal-processing framework for inverse rendering. *ACM Transactions on Graphics*, 2001. 2, 3, 4
- [25] Mike Roberts, Jason Ramapuram, Anurag Ranjan, Atulit Kumar, Miguel Angel Bautista, Nathan Paczan, Russ Webb, and Joshua M. Susskind. Hypersim: A photorealistic synthetic dataset for holistic indoor scene understanding. In *Proceedings of the IEEE/CVF International Conference on Computer Vision (ICCV)*, 2021. 2, 6
- [26] Pratul P Srinivasan, Boyang Deng, Xiuming Zhang, Matthew Tancik, Ben Mildenhall, and Jonathan T Barron. NeRV: Neural Reflectance and Visibility Fields for Relighting and View Synthesis. In *Proceedings of the IEEE/CVF Conference on Computer Vision and Pattern Recognition*, pages 7495–7504, 2021. 2
- [27] Jianyuan Wang, Minghao Chen, Nikita Karaev, Andrea Vedaldi, Christian Rupprecht, and David Novotny. Vggt: Visual geometry grounded transformer. In *Proceedings of the IEEE/CVF Conference on Computer Vision and Pattern Recognition*, 2025. 2, 3, 7, 8

[28] Yifan Wang, Jianjun Zhou, Haoyi Zhu, Wenzheng Chang, Yang Zhou, Zizun Li, Junyi Chen, Jiangmiao Pang, Chunhua Shen, and Tong He. Pi 3: Permutation-equivariant visual geometry learning. *arXiv preprint arXiv:2507.13347*, 2025. 3

[29] Lihe Yang, Bingyi Kang, Zilong Huang, Zhen Zhao, Xiaogang Xu, Jiashi Feng, and Hengshuang Zhao. Depth anything v2. *arXiv:2406.09414*, 2024. 7, 8

[30] Alex Yu, Vickie Ye, Matthew Tancik, and Angjoo Kanazawa. pixelnerf: Neural radiance fields from one or few images. In *Proceedings of the IEEE/CVF Conference on Computer Vision and Pattern Recognition (CVPR)*, 2021. 3

[31] Zheng Zeng, Valentin Deschaintre, Iliyan Georgiev, Yannick Hold-Geoffroy, Yiwei Hu, Fujun Luan, Ling-Qi Yan, and Milos Hasan. Rgb↔x: Image decomposition and synthesis using material- and lighting-aware diffusion models. In *SIGGRAPH (Conference Paper Track)*, page 75. ACM, 2024. 3, 8

[32] Jingsen Zhang, Shunsuke Saito, and Matthias Nießner. Neilf: Neural incident light field for material and lighting estimation. In *Proceedings of the European Conference on Computer Vision (ECCV)*, 2022. 2

[33] Kai Zhang, Fujun Luan, Qianqian Wang, Kavita Bala, and Noah Snavely. Physg: Inverse rendering with spherical gaussians for physics-based material editing and relighting. In *Proceedings of the IEEE/CVF Conference on Computer Vision and Pattern Recognition*, pages 5453–5462, 2021.

[34] Xiuming Zhang, Pratul P Srinivasan, Boyang Deng, Paul Debevec, William T Freeman, and Jonathan T Barron. NeRFactor: Neural Factorization of Shape and Reflectance Under an Unknown Illumination. *ACM Transactions on Graphics (ToG)*, 40(6):1–18, 2021.

[35] Yuanqing Zhang, Jiaming Sun, Xingyi He, Huan Fu, Rongfei Jia, and Xiaowei Zhou. Modeling Indirect Illumination for Inverse Rendering. In *Proceedings of the IEEE/CVF Conference on Computer Vision and Pattern Recognition*, pages 18643–18652, 2022. 2

[36] Tinghui Zhou, Philipp Krähenbühl, and Alexei A. Efros. Learning data-driven reflectance priors for intrinsic image decomposition. In *Proceedings of the IEEE International Conference on Computer Vision (ICCV)*, 2015. 3

[37] Jingsen Zhu, Fujun Luan, Yuchi Huo, Zihao Lin, Zhihua Zhong, Dianbing Xi, Rui Wang, Hujun Bao, Jiaxiang Zheng, and Rui Tang. Learning-based inverse rendering of complex indoor scenes with differentiable monte carlo raytracing. In *SIGGRAPH Asia*, pages 6:1–6:8. ACM, 2022. 3

[38] Jingsen Zhu, Fujun Luan, Yuchi Huo, Zihao Lin, Zhihua Zhong, Dianbing Xi, Rui Wang, Hujun Bao, Jiaxiang Zheng, and Rui Tang. Learning-based inverse rendering of complex indoor scenes with differentiable monte carlo raytracing. In *SIGGRAPH Asia 2022 Conference Papers*. ACM, 2022. 6

[39] Rui Zhu, Zhengqin Li, Janarbek Matai, Fatih Porikli, and Manmohan Chandraker. Irisformer: Dense vision transformers for single-image inverse rendering in indoor scenes. In *Proceedings of the IEEE/CVF Conference on Computer Vision and Pattern Recognition*, pages 2822–2831, 2022. 3

[40] Dong Zhuo, Wenzhao Zheng, Jiahe Guo, Yuqi Wu, Jie Zhou, and Jiwen Lu. Streaming 4d visual geometry transformer. *arXiv preprint arXiv:2507.11539*, 2025. 3